NATIONAL TRANSPORTATION SAFETY BOARD
Office of Research and Engineering
Vehicle Performance Division
Washington, D.C. 20594

August 3, 2017

Finite Element Modeling Study Report

A. ACCIDENT INFORMATION

Place	:	New Martinsville, West Virginia
Date	:	August 27, 2016
Vehicle	:	AXLX 1702 Liquid Chlorine Tank Car
NTSB No.	:	DCA16SH002
Investigator	:	Paul Stancil

B. TOPICS ADDRESSED

Finite element (FE) modeling was used to examine local stresses in the tank near the nose of the cradle pad caused by the local geometry of the weld.

C. DETAILS OF THE STUDY

3-D finite element models of the tank car were constructed. The focus was on the region near the cradle pad nose. Four cases of weld geometries were studied for their effects on local stresses. The FE modeling was carried out using the FE software Abaqus version R2016x.

1. Geometry

The geometry of the tank car was mainly based on design drawings [Reference 1]. An FE model of a different type tank car, provided by the Volpe Transportation Systems Center, was used as reference. Figure 1 shows the geometry of the assembled tank car model. Half of the tank car assembly was modeled to take advantage of the symmetry. Modeled parts included the tank, the cradle pad, the bolster structure, and the stub sill plate. Figures 2 through 4 show the geometry of the cradle pad, the bolster structure and the stub sill plate, respectively.

2. Material

The tank was made from AAR TC-128 Grade B carbon steel. The other parts were made of ASTM A-572 type steel. For details on the tank car material, please refer to Reference 2. In the FE model, a linear elastic material model was used for all steel materials with a Young's modulus of 29,000 ksi and a Poisson's ratio of 0.3.

3. Loads and Boundary Conditions

Loads simulating a loaded tank car were applied to the model. The gross weight for the tank car AXLX 1702 was 261,950 lbs. This weight was applied as a uniformly distributed load in the downward direction to the interior surface of the tank. The tank car was also loaded to an internal pressure of 65 psi. This pressure was applied to the interior surface of the tank as a pressure load.

To simulate the boundary condition of the tank car sitting on trucks, a reference point was first created at the center line of the pin. A kinematic coupling constraint was then created linking the reference point to regions on the stub sill flanges representing fastening locations. Figure 5 shows this coupling constraint. Simple support boundary conditions were applied to the reference point. In addition, symmetric boundary conditions were applied at the half-symmetry plane of the tank car.

With the exception of cradle pad welds (discussed in the next section), the weld geometry between different parts was not included in the FE model. Instead, mesh tie constraints were created to simulate the welds.

4. Modeling of the Cradle Pad Welds

The FE model included the geometry of the weld of the cradle pad to the tank shell. Figure 6 shows the local region of the cradle pad with the weld, and Figure 7 shows a cross section of the plate with the weld.

Four different weld geometries were considered and are shown in Figures 8 and 9. The first case, called the “wrap-around case”, had the two ends of the weld separated by 8 inches. This was based on the specification of an 8-inch no-weld zone [Reference 1]. The second case, called the “45-degree case”, had each side of the weld terminated at about 45-degrees as the weld went around the corner of the cradle plate nose. The third case, called the “shorter case”, has the weld terminating approximately one inch short of the 45-degree location. The fourth case, called the “asymmetric case”, has one side of the weld resembling the “wrap-around case” and the other side resembling the “shorter case”. In the fourth case, the geometry of the cradle pad nose was also modified to have a ¼ inch corner fillet radius to be closer to the cradle pad found on the accident train. For each case, the weld was rounded at its termination. Mesh tie constraints were created at both the weld-pad and weld-tank interfaces to simulate the weld interface.

5. Mesh

The majority part of the tank car assembly was meshed with quadrilateral shell elements (S4R in Abaqus). The cradle pad was meshed with brick solid elements (C3D8R in Abaqus). The cradle pad to tank shell welds were meshed with mixed brick and 2nd-order tetrahedral solid elements (C3D10 in Abaqus). A portion of the tank in the vicinity of the cradle pad nose, shown in Figure 10 using the wrap-around case as an example, was also meshed with brick solid elements to study the through-thickness stress distribution. Mesh tie constraints or Shell-to-solid coupling constraints were created at the

interface between shell elements and solid elements for smooth transition. Figure 11 shows the FE mesh in the region near the nose of the cradle pad, again using the wrap-around case as an example. The tank mesh near the tip of the cradle pad was refined to have a typical size of 0.2 inches. Mesh sizes for the rest of the model are summarized in Table 1.

Table 1.Mesh statistics for the FE model

Part name	**Element type**	**Number of elements**	**Typical mesh size (inch)**
Cradle pad	Solid	56,657	1, with 3 elements through thickness
Cradle pad weld (wrap-around case)	Solid	22,234	0.2
Bolster structure	Shell	8,800	1
Stub sill	Shell	5,455	1
Tank	Shell and solid	249,238	5, locally refined to 0.2

6. Output

Figures 12 and 13 show the maximum principal stress and the Mises stress distributions near the cradle pad nose region for the asymmetric weld case. A stress concentration can be observed on the tank shell near the corner of the cradle pad. The magnitudes of the local stresses introduced by the weld termination were approximately 12 ksi (maximum principal stress) and 10 ksi (Mises stress). The local stresses were approximately the same at each side of the asymmetric weld terminations. Figure 14 compares the longitudinal (S33) and the horizontal (S11) component of the stress in the part of the tank modeled with solid elements. The longitudinal stress component displays a higher magnitude, indicating the more dominating deformation mode of the tank is bending due to the weight as opposed to expansion due to the internal pressure. Figure 15 shows the through-thickness maximum principal stress distribution at the location of the weld termination on the wrap-around side. Figures 16 and 17 compare the maximum principal stress and the Mises stress distributions on the tank shell for all four weld cases. All four cases displayed stress concentrations of similar magnitudes (and also similar to those in Figures 12 and 13). For the wrap-around weld case and the 45-degree weld case, the stress concentrations were located near the corner of the cradle pad. For the shorter weld case, the stress concentrations were located further away from the cradle pad nose, near where the welds were terminated.

D. REFERENCES

1. Tank car design drawings, ACF Industries.
2. Materials Laboratory Factual Report No. 17-001, 2017.

Xiaohu Liu
Finite Element Analyst

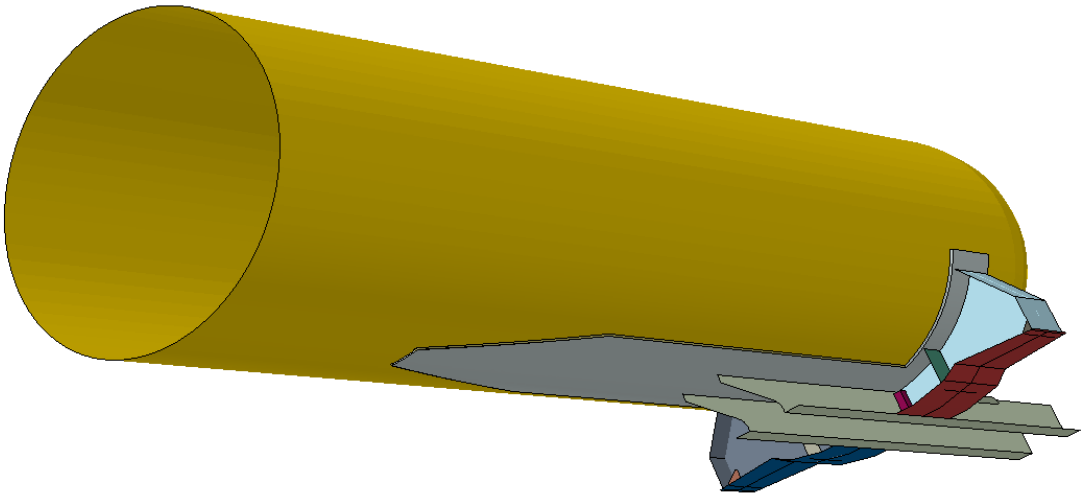

Figure 1. Geometry of the assembled tank car model.

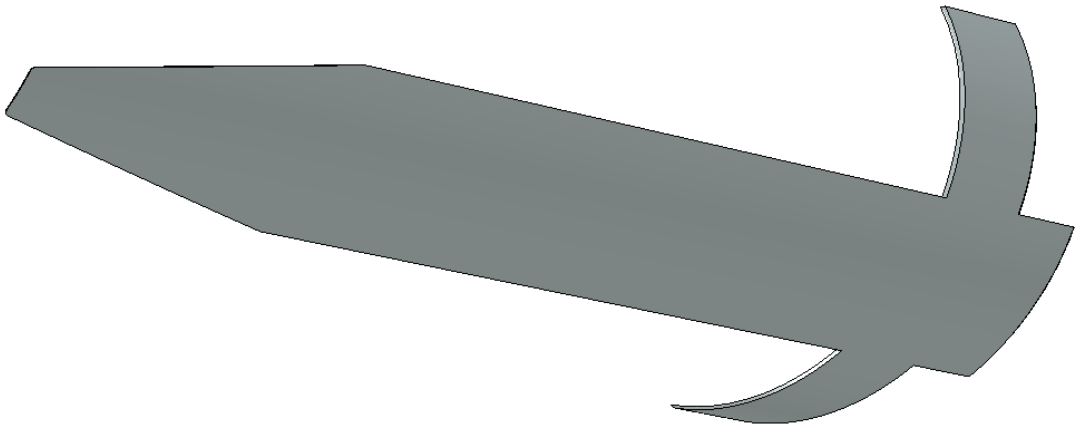

Figure 2. Geometry of the cradle pad.

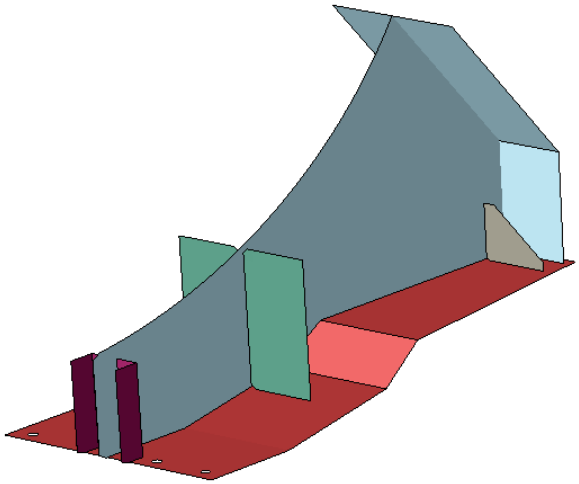

Figure 3. Geometry of the bolster structure (one side only).

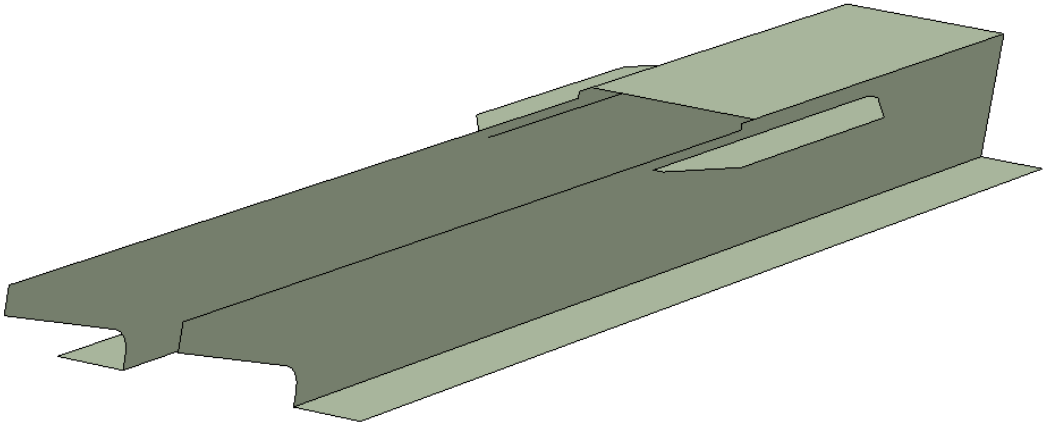

Figure 4. Geometry of the stub sill plate.

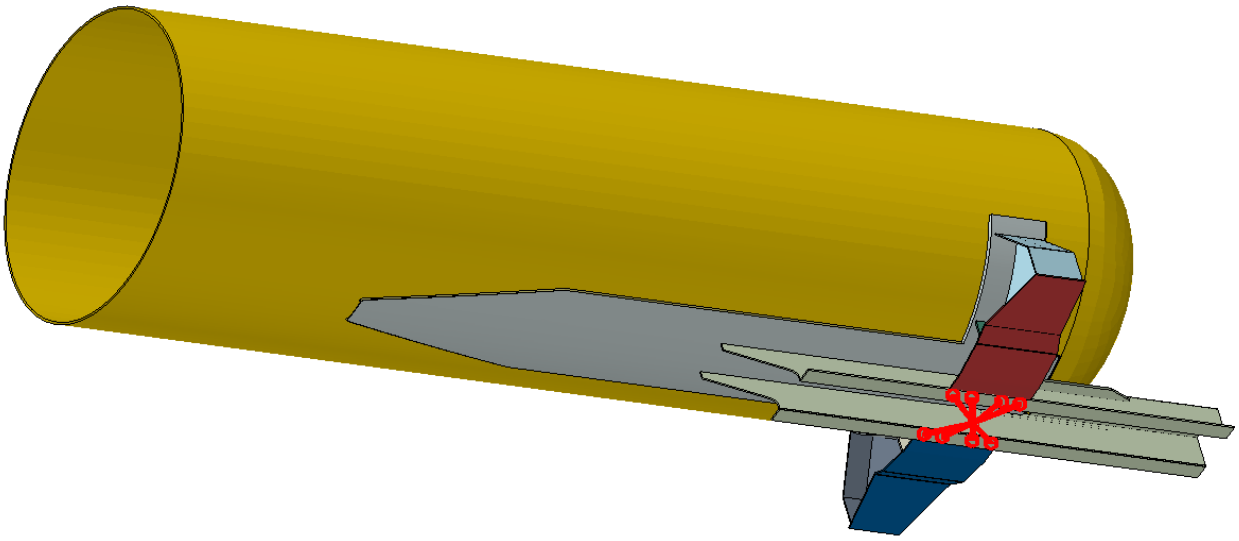

Figure 5. Kinematic coupling constraint simulating the tank car sitting on a truck.

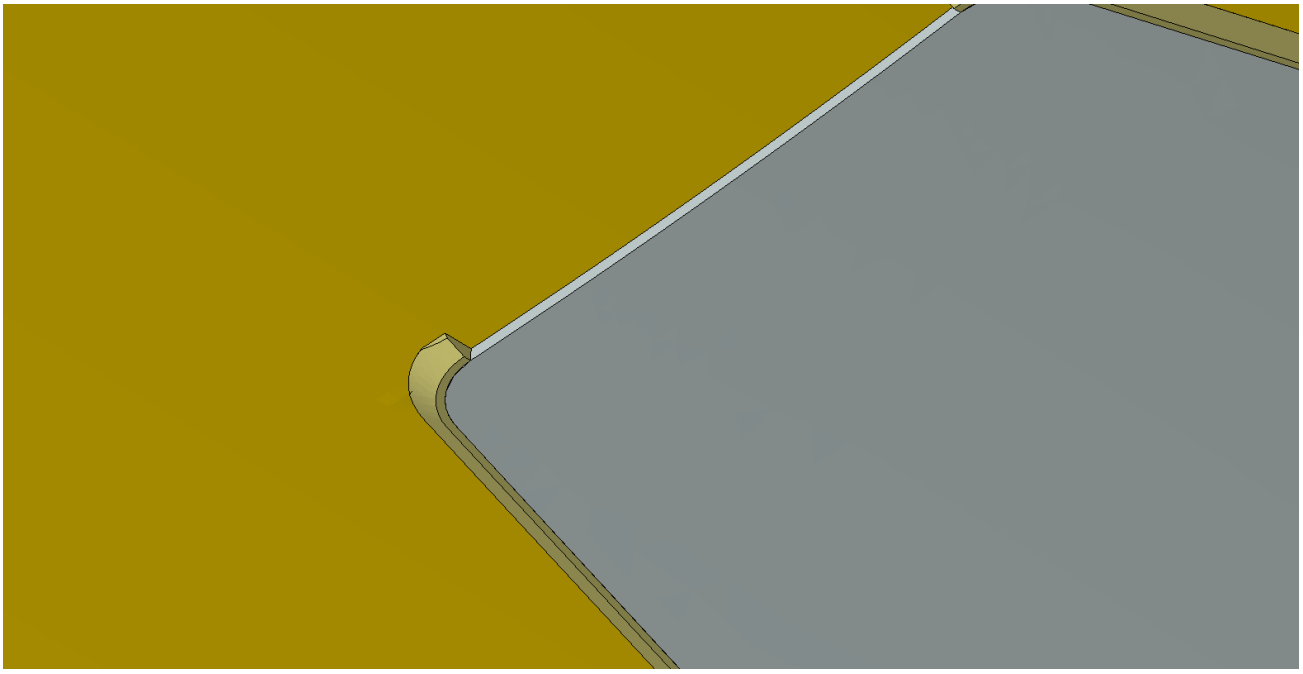

Figure 6. Weld geometry near the cradle pad nose, wrap-around weld case.

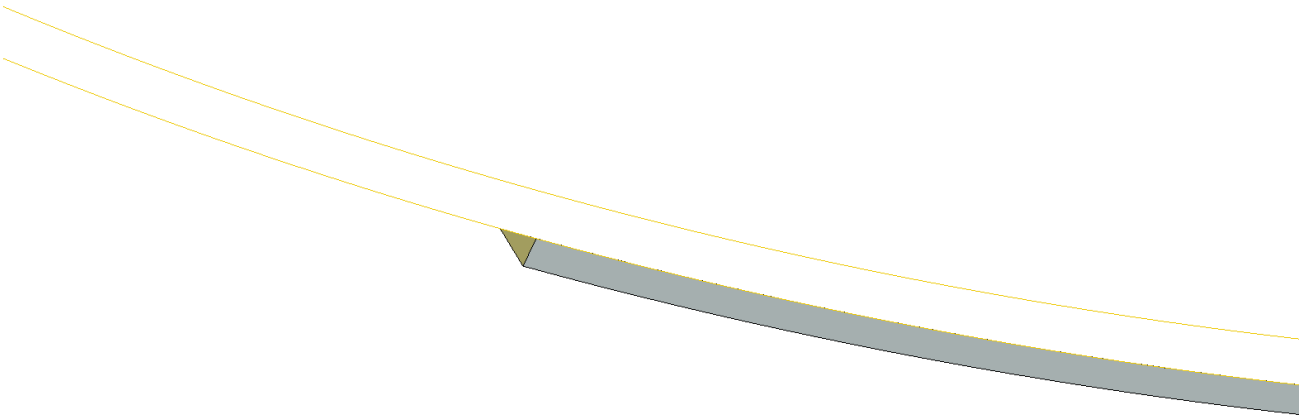

Figure 7. A cross section containing the tank shell, cradle pad and the cradle pad weld.

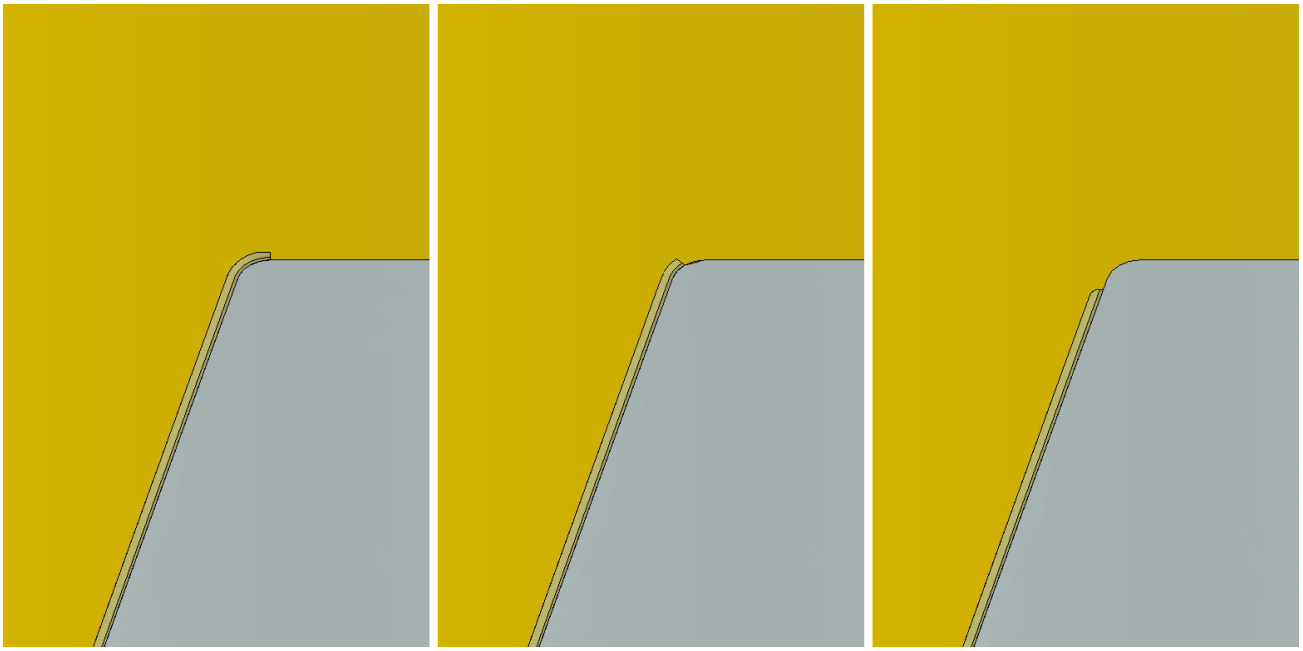

Figure 8. The first three weld geometries studied: Wrap-around (left), 45-degree (middle) and Shorter (right).

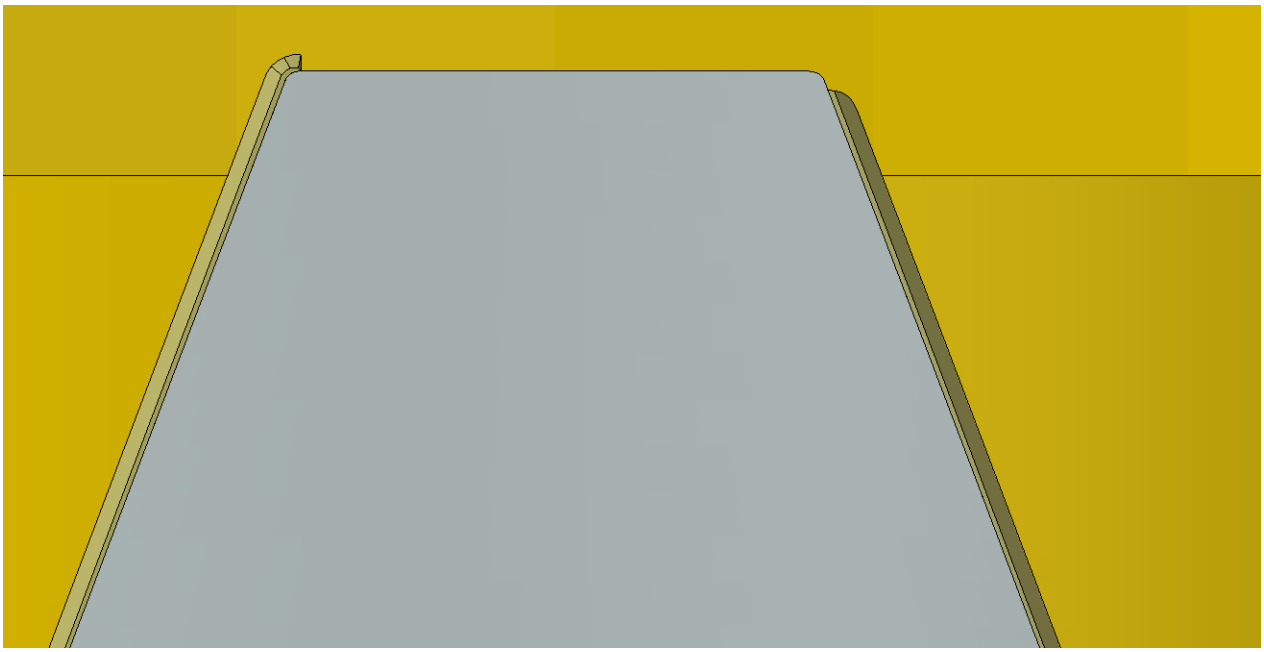

Figure 9. Weld geometry for the asymmetric case.

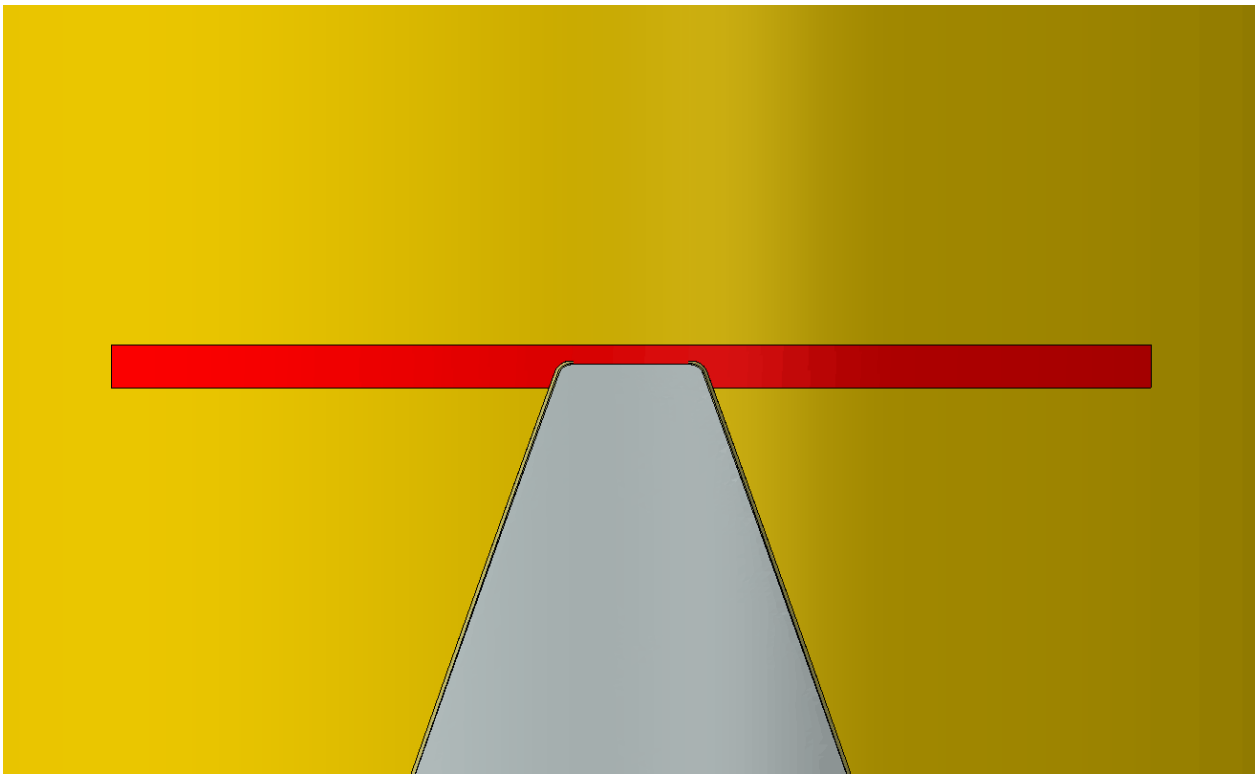

Figure 10. The tank region (shown in red) modeled with solid elements.

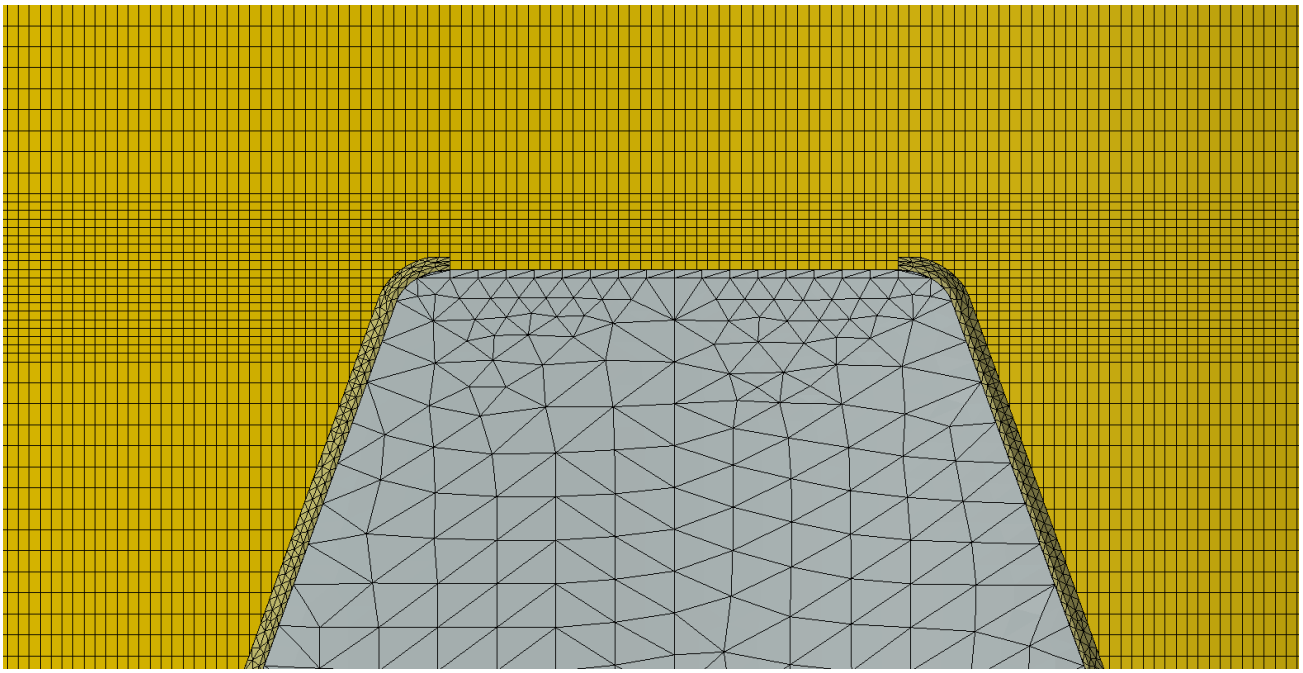

Figure 11. FE mesh near the cradle pad nose.

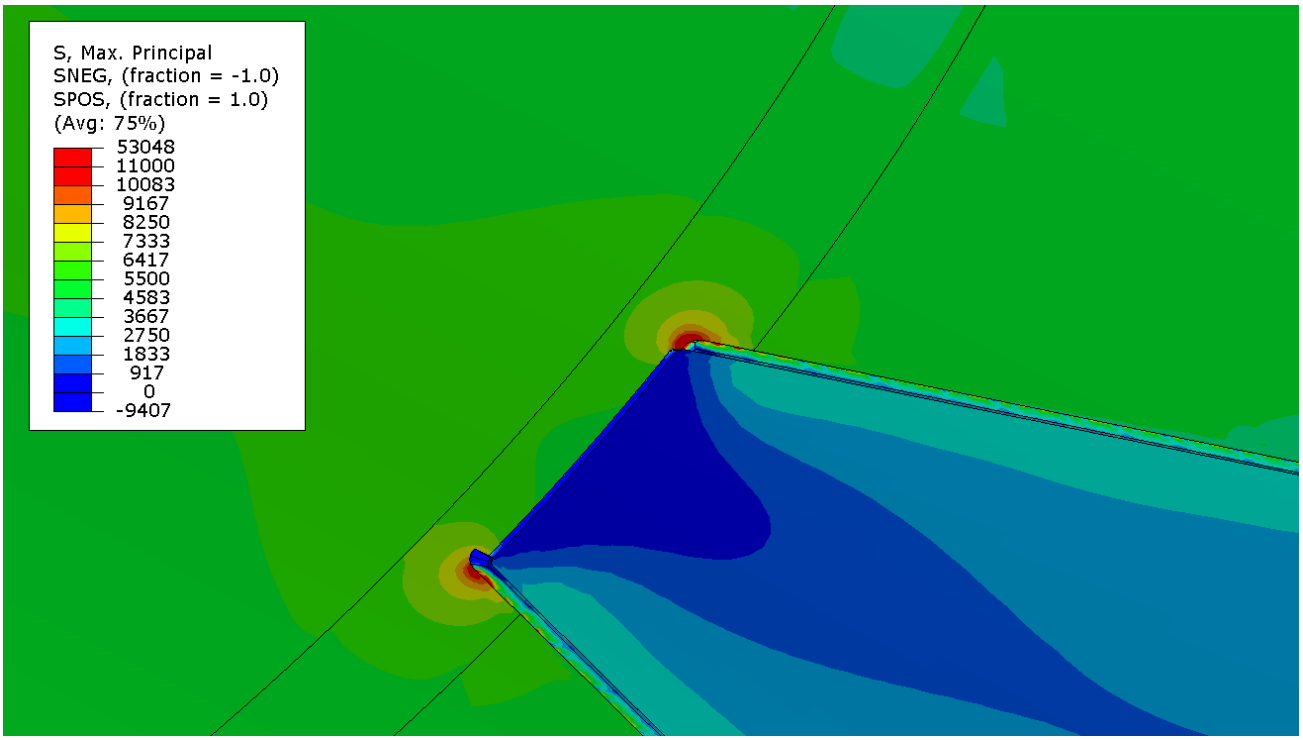

Figure 12. Maximum principal stress distribution near the cradle pad nose (asymmetric weld case).

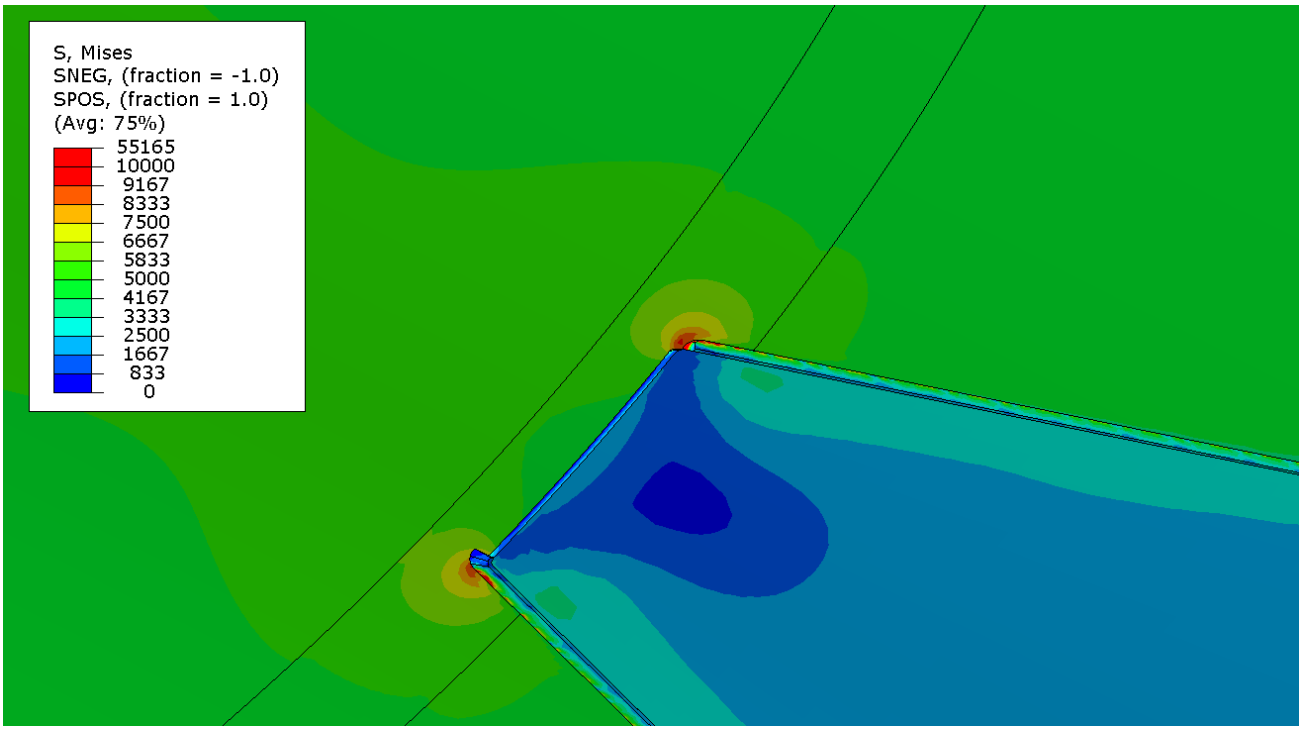

Figure 13. Mises stress distribution near the cradle pad nose (asymmetric weld case).

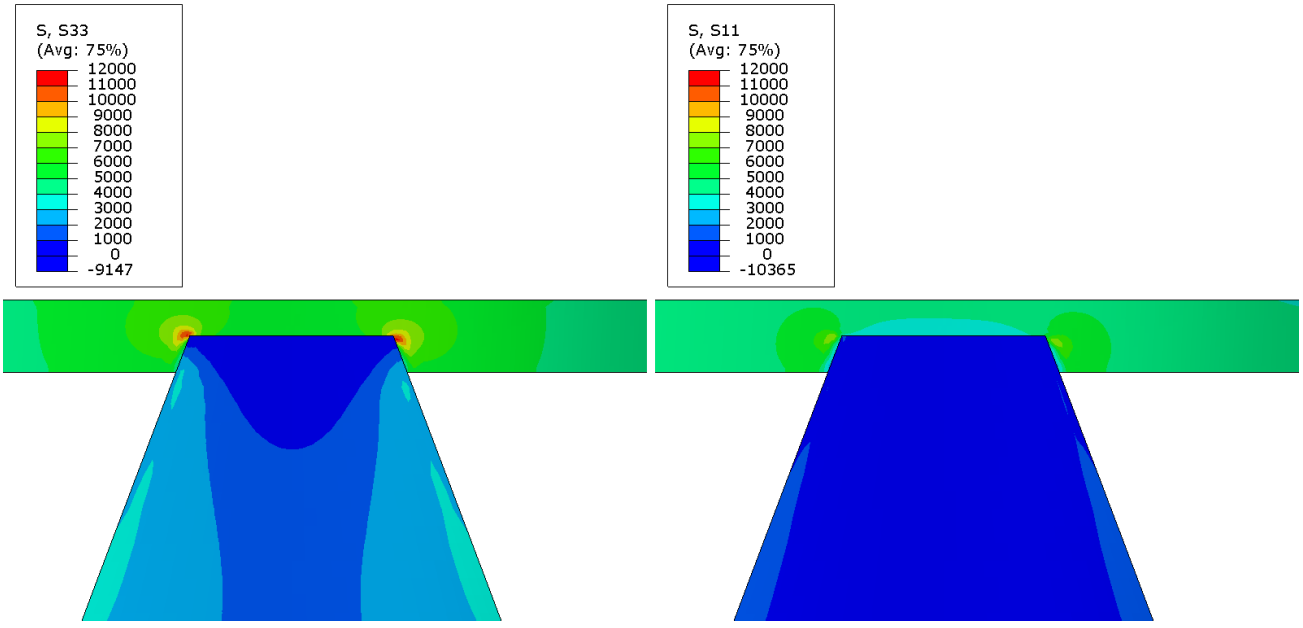

Figure 14. Comparison of the longitudinal (left) and horizontal (right) stress component in the tank region modeled with solid elements.

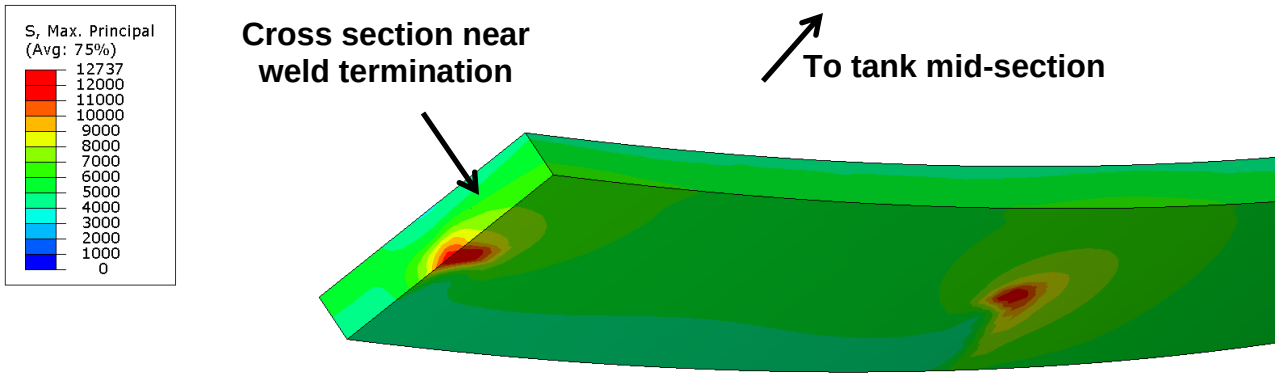

Figure 15. Maximum principal stress distribution on the cross section of the tank region modeled with solid elements.

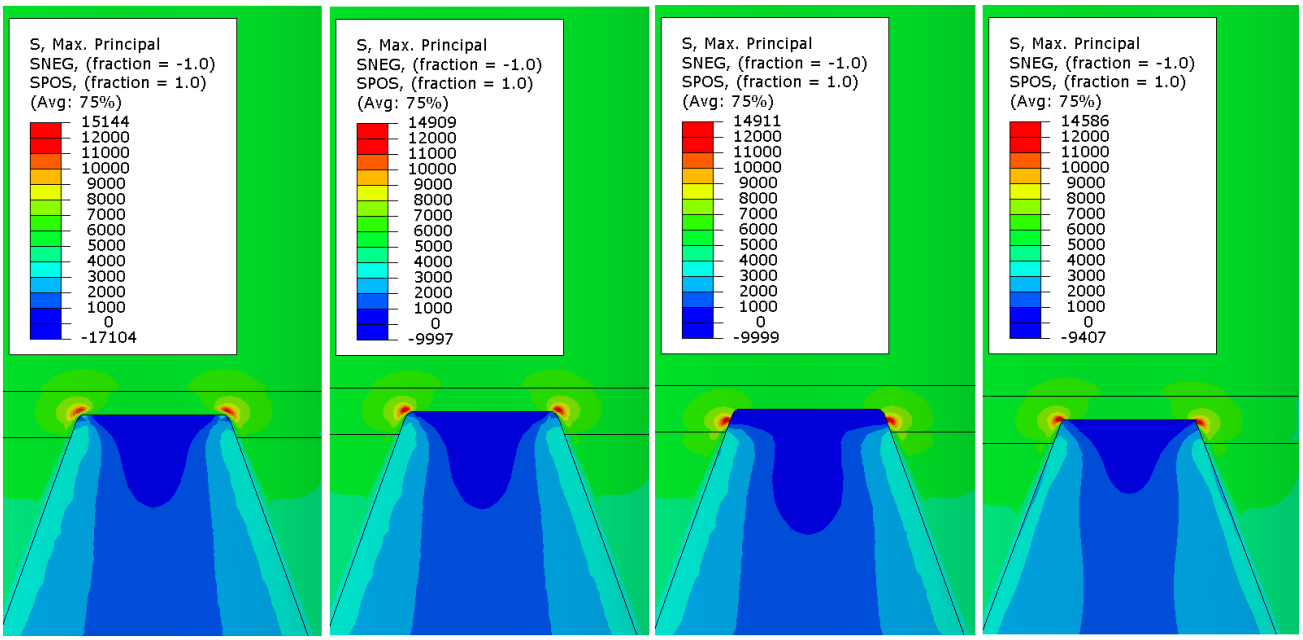

Figure 16. Maximum principal stress distribution near the cradle pad nose, comparison of four weld geometry cases.

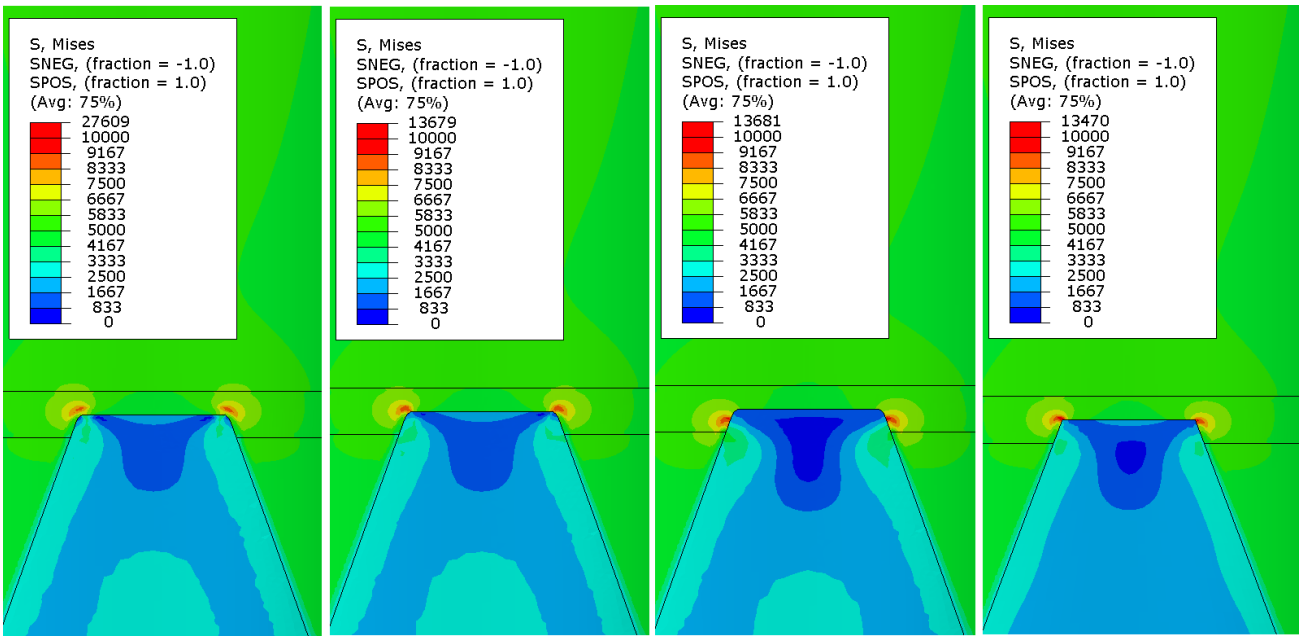

Figure 17. Mises stress distribution near the cradle pad nose, comparison of four weld geometry cases.